학 사 학 위 논 문

딥 러닝을 이용한 $t\bar{t}b\bar{b}$ 과정에서의 b-jet 식별 연구

Study of Identification of b-jets in the $t\bar{t}b\bar{b}$ Process Using Deep Learning

임 종 원

한 양 대 학 교

2020년 2월

학 사 학 위 논 문

딥 러닝을 이용한 $t\bar{t}b\bar{b}$ 과정에서의 b-jet 식별 연구

Study of Identification of b-jets in the $t\bar{t}b\bar{b}$ Process Using Deep Learning

지도교수 김 태 정

이 논문을 이학 학사학위논문으로 제출합니다.

2020년 2월

한 양 대 학 교

물 리 학 과

임 종 원

이 논문을 임종원의 이학 학사학위 논문으로 인준함.

2020년 2월

지도교수 (인)

심사위원 (인)

한 양 대 학 교

초록

LHC (Large Hadron Collider) 에서는 입자 충돌 실험을 통해 입자의 생성과 붕괴 과정을 연구한다. 탑 쿼크의 붕괴 과정 중 하나인 $t\bar{t}b\bar{b}$ 과정에서는 글루온으로부터 추가적인 b-jet이 나온다. 검출기에서 검출되는 b-jet 중에서 글루온으로부터 온 b-jet을 운동학적 성질을 이용하여 식별한다. 이 연구에서는 기존의 가장 작은 ΔR을 형성하는 두 개의 b-jet 으로부터 추가적인 b-jet임을 식별하는 방법과 다르게, 딥 러닝을 이용하여 추가적인 b-jet을 식별하고자 한다. 딥 러닝을 사용했을 때 얼마나 더 잘 식별할 수 있는지를 보고자 한다.

Abstract

In LHC (Large Hadron Collider) collision experiment, protons collide and lots of particles are created and annihilated. The $t\bar{t}b\bar{b}$ process is the one of the decay processes of top quark and there are additional b-jets from gluon. We identify reconstructed b-jets which are from the additional b-jets using kinematic properties of b-jets from gluon. Traditionally, we identify the additional b-jets with two b-jets whose ΔR is minimum. In this study, we use deep learning to identify the additional b-jets and expect to get better performance than the traditional method.

Contents

1 Introduction

1.1 Particle Physics and the Standard Model

Particle Physics is a study about mechanism of fundamental particles. The very start of the experimental particle physics is concerned as the discovery of electron by J.J. Thomson. In 1980s, the theory of the Standard Model was completed. In 2012, the standard model has been completely proved with the discovery of Higgs boson.

The Standard Model is consisted of quarks, leptons, gauge bosons and Higgs boson. There are 6 kinds of quarks and they are fermions whose spin is half integer. Likewise, leptons are fermions and they are consisted of electron, muon, tau and their neutrinos. Photon, gluon, W and Z boson are force carrier. Photon and gluon carry electromagnetic interaction and strong force respectively. W and Z boson mediate weak interaction. Higgs boson gives mass to particles in the form of interaction with Higgs field.

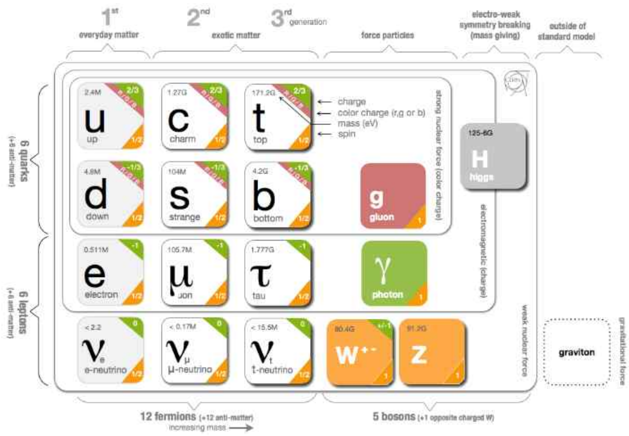

Figure 1.1 The Standard Model [1]

1.2 CERN and LHC

Experiments of particle physics on these days are mostly particle collision experiments. CERN (Conseil Européenne pour la Recherche Nucléaire) is one of the institutes that collision experiments are held. CERN is located at the border of Switzerland and France. In CERN, there is the world largest particle accelerator, LHC (Large Hadron Collider) which accelerates the protons up to 6.5 TeV per beam [2]. LHC is placed 100 m below ground level and its circumference is about 27 km. The accelerated beams collide at four detectors - CMS, ATLAS, ALICE, LHCb - where the total energy at the collision point is equal to 13 TeV.

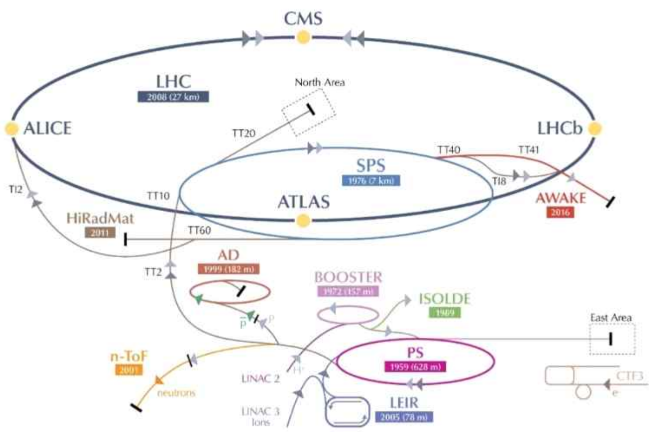

Figure 1.2 CERN and LHC [3]

1.3 CMS Detector

CMS (Compact Muon Solenoid) is 21 meters long, 15 meters wide, and 15 meters high [4]. CMS is composed of 4 detector layers - Tracking chamber, ECAL (Electromagnetic Calorimeter), HCAL (Hadron Calorimeter), Muon chamber from innermost (Figure 1.3). Tracking chamber detects particles with electric charge. In ECAL and HCAL, particles will decay due to their energy loss. Particles interacting with electromagnetic field decay in ECAL, and hadrons which are composed of quarks decay in HCAL. The Muon chamber, the outermost part, detects muons with the longest lifetime among unstable particles.

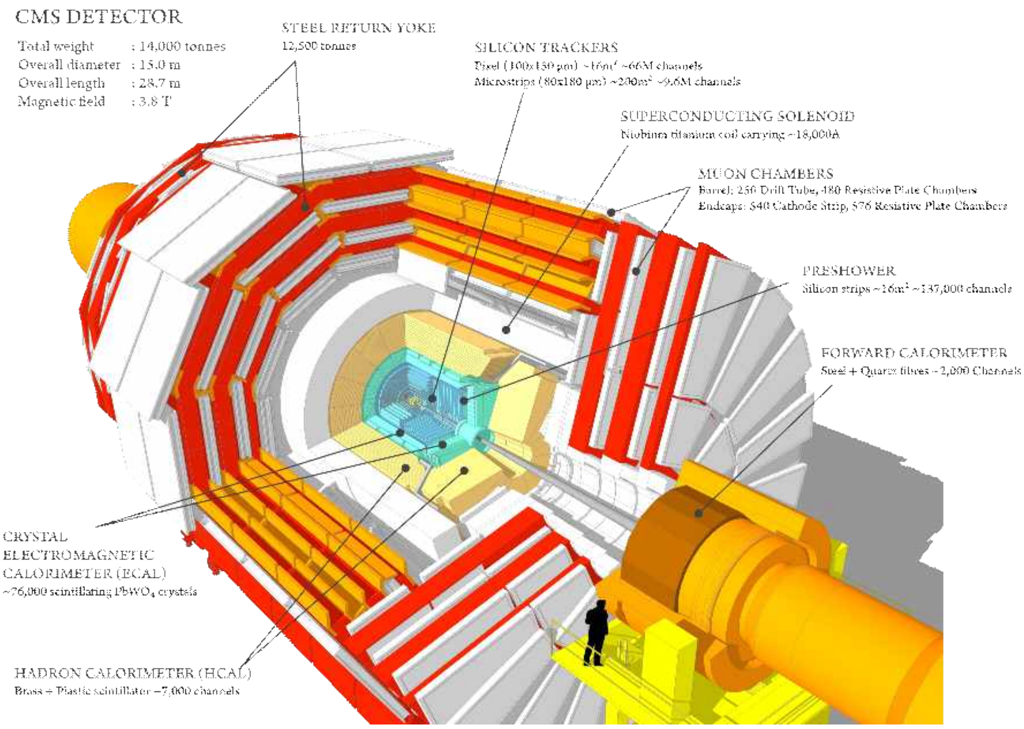

Figure 1.3 CMS Detector [5]

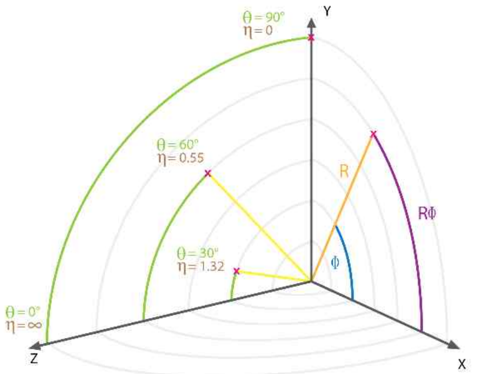

Figure 1.4 Detector Coordinates [6]

In Figure 1.4, detector coordinate is described. z-direction is the proton beam direction. Pseudo-rapidity η and azimuthal angle ϕ are defined in (1.1). The anglular distance, ΔR defined in (1.2), which is invariant under longitudinal boost is used for describing jet's shape.

$$\eta \equiv -ln\left[tan\left(\frac{\theta}{2}\right)\right] \tag{1.1}$$

$$\Delta R \equiv \sqrt{(\Delta\eta)^2 + (\Delta\phi)^2} \tag{1.2}$$

2 Event Sample

2.1 The $t\bar{t}b\bar{b}$ process

Top quark has the heaviest mass of 173 GeV in the Standard Model. In LHC, with the center of mass collision energy of 13 TeV, several top quark decay processes are produced. One of the processes is the $t\bar{t}H(b\bar{b})$ process, and its major background process is the $t\bar{t}b\bar{b}$ process (Figure 2.1). The $t\bar{t}H(b\bar{b})$ process is important to understanding the interaction between top quark and Higgs boson. Also, for studying FCNC (Flavor Changing Neutral Current), the $t\bar{t}b\bar{b}$ event is the main background of $tcH(b\bar{b})$ event. To clarify the signal, the background process should be clearly classified. Therefore, understanding about the $t\bar{t}b\bar{b}$ process is crucial.

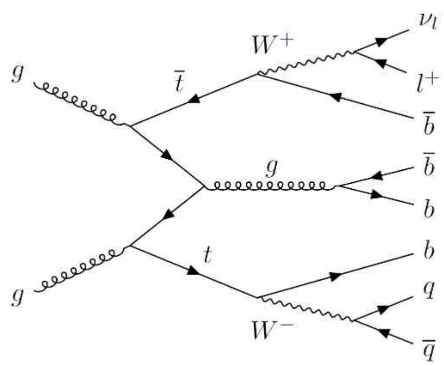

Figure 2.1 The $t\bar{t}b\bar{b}$ process

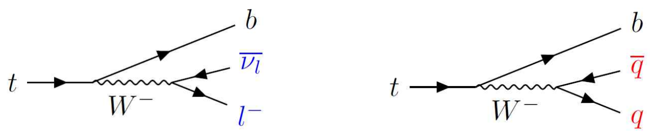

Figure 2.2 Top quark decay modes (Leptonic (left) and Hadronic (right) decay)

Top quark mostly decays into W boson and b-quark (bottom quark) and W boson decays into two decay modes. One is hadronic decay mode, and the other is leptonic decay mode. W boson decays into quark and anti-quark in hadronic decay mode, and lepton and its neutrino in leptonic decay mode (Figure 2.2). In the $t\bar{t}b\bar{b}$ process, there are two W bosons in the intermediate states, thus there are three different channels; lepton + jets channel, dileptonic channel and hadronic channel. In this study, we will focus on lepton + jets channel which has one hadronic and one leptonic decay mode of W boson.

The $t\bar{t}b\bar{b}$ process has 6 jets in the final state. Among the jets, there are additional b-jets from gluon, and we will identify them as a signal of the $t\bar{t}b\bar{b}$ process. Other jets are originated from top quark or hadronic decay of W boson. Additional b-jets has smaller ΔR than other b-jets since their QCD interaction of gluon splitting [7].

2.2 Event Simulation

In this study, we used simulated events, not real experimental data. By using event generator, we made event samples similar with experimental data. In the CMS detector, the particle collides each other and undergoes detector effects. There are three steps for the event simulation, matrix element calculation, parton shower, and fast detector simulation. For each step, there are corresponding event generator. MadGraph [8] and MadSpin [9] is used to calculate matrix element which relates the initial and final states of the particle decay process.

Pythia [10] is responsible for a parton shower (hadronization process). Monte Carlo method is used in Pythia since hadronization process is totally random. Jets are produced after hadronization and they enter detector simulation. Delphes [11] is used for the final step, fast detector simulation. Through Delphes, we obtain reconstructed data as like from the CMS detector. There are two levels in terms of detector. Generated level is the same with particle level before the hadronization. After hadronization, generated level particles enter the detector and we reconstruct particle with electronic signals from the detector in reconstruction level.

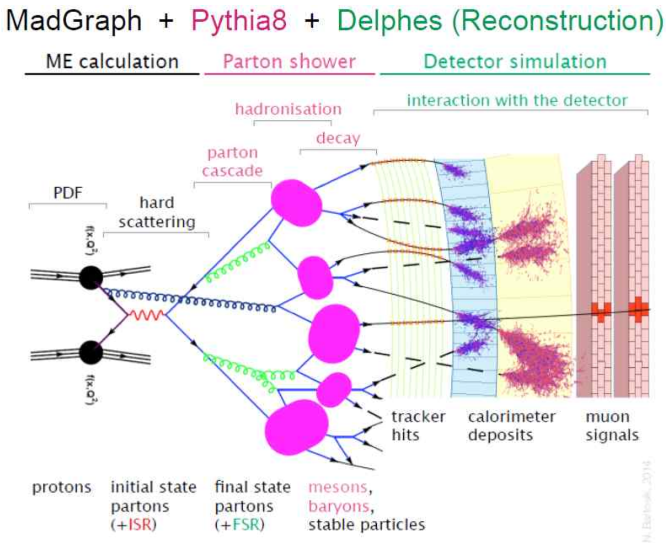

Figure 2.3 Event Simulation Stages and Tools [12]

2.3 Event Selection

Event selection is needed to remove unrealistic events in event simulation sample. Here, we define signal as two additional b-jets from the $t\bar{t}b\bar{b}$ process. For the signal definition (Selection 1), we require transverse momenta $p_T \geq 20$ GeV and absolute pseudo-rapidity $|\eta| \leq 2.5$ of generated jets. There are two objects to be selected, a lepton and jets. For lepton (Selection 2), electron and muon are selected whose $p_T \geq 30$ GeV and $|\eta| \leq 2.4$ in both electron and muon. Jets should have $p_T \geq 30$ GeV and $|\eta| \leq 2.5$ (Selection 3) [13].

Signal Definition	Selection 1	Generated Jets	$p_T \geq 20, \lvert\eta\rvert \leq 2.5$
Object Selection	Selection 2	Lepton (Electron, Muon)	$p_T \geq 30, \lvert\eta\rvert \leq 2.4$
	Selection 3	Jets	$p_T \geq 30, \lvert\eta\rvert \leq 2.5$

Table 2.1 Event Selection

The $t\bar{t}b\bar{b}$ process has four b-jets in the final states and two jets from leptonic decay of W boson, therefore we need to require at least 6 jets and 4 b-jets. However, in this study, we will vary the required number of jets and b-jets and look at the tendency of the performance. We generated 10 million events at event simulation process. In Table 2.2, there are 12 event selections and corresponding number of selected events.

The number of events after the three steps of selection is the total number of selected events for the further analysis.

Number of Jets	Number of b-Jets	Number of Events after Selections		
		Selection1 (Gen. jets)	Selection2 (Lepton)	Selection3 (Jets)
≥ 2	≥ 2	1888043	561273	275117
	≥ 3			273659
	≥ 4			259712
	≥ 5			213440
	≥ 6			137136
≥ 3	≥ 3			91961
	≥ 4			90187
	≥ 5			79489
	≥ 6			55439
≥ 4	≥ 4			15329
	≥ 5			14638
	≥ 6			11478

Table 2.2 The Number of Selected Events with Various Event Selections

3 Identification of Two Additional b-Jets

Identifying additional b-jets is a process of identifying the process. We will identify two additional b-jets using two different method, Minimum ΔR method and Deep Learning method. Reconstruction efficiency is an important measurement of identifying additional b-jets. It is the ratio between the matched events and total events. The definition of matching is different in two different methods. However, the meaning of the efficiency is the same as the performance of identifying additional b-jets.

3.1 Minimum ΔR Method

In terms of the generated additional b-jets, ΔR of them is relatively smaller than that of other b-jets. Using this kinematics, when we select minimum ΔR of two reconstructed b-jets, they will have a chance to be the additional b-jets. Due to the ΔR of a jet is set to 0.4, if ΔR between the reconstructed b-jet and generated additional b-jet is smaller than 0.4, they are matched as additional b-jets. In table 3.1, there are reconstruction efficiencies under different selections.

Number of Jets	Number of b-Jets	Matched Events	Total Events	Reconstruction efficiency (%)
≥ 2	≥ 2	58172	275117	21.14
	≥ 3	57844	273659	21.14
	≥ 4	54945	259712	21.16
	≥ 5	45090	213440	21.13
	≥ 6	28833	137136	21.03
≥ 3	≥ 3	26394	91961	28.70
	≥ 4	25860	90187	28.67
	≥ 5	22585	79489	28.41
	≥ 6	15448	55439	27.86
≥ 4	≥ 4	4641	15329	30.28
	≥ 5	4388	14638	29.98
	≥ 6	3344	11478	29.13

Table 3.1 Reconstruction Efficiencies under various Event Selections

At Table 3.1, reconstruction efficiency increases when we require tighter selection of the number of b-jets. Loose selections such as the number of jets ≥ 2 have much more background events than signal events with low reconstruction efficiency. For this reason, when we require at least 4 jets, we could get the highest reconstruction efficiencies.

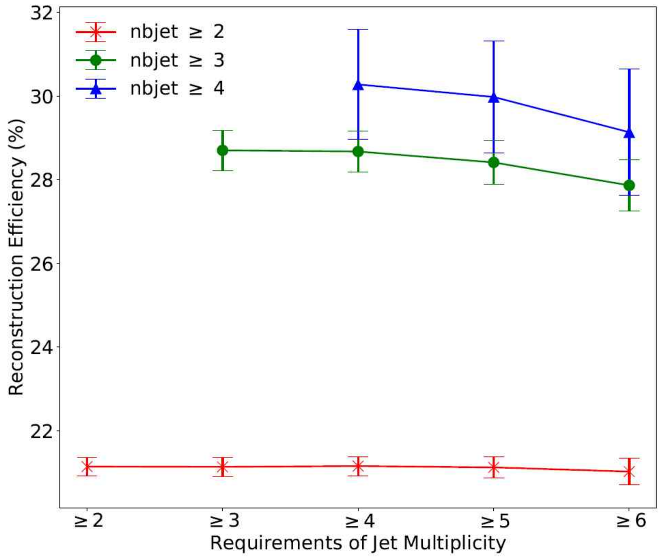

Figure 3.1 Plot of Reconstruction Efficiencies under various Event Simulations

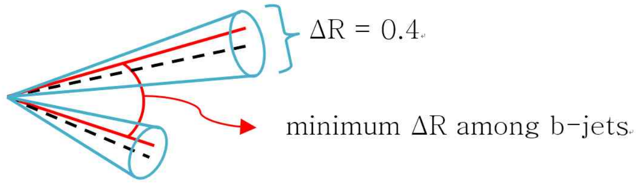

Figure 3.2 Matching mechanism : If ΔR of generated additional b-jets (dashed line) and reconstructed b-jets (solid line) are less than 0.4, or within the cone, then generated level additional b-jets and reconstruction level b-jets are matched. As we choose reconstructed b-jets, their ΔR is the minimum among other b-jets combinations.

3.2 Deep Learning Method

Deep learning method is a modern way of using Deep Neural Network (DNN) to identify additional b-jets. Unlike minimum ΔR method, deep learning is useful for multivariate analysis which is requires many input variables. Input variables used for deep learning are listed in Appendix 1.

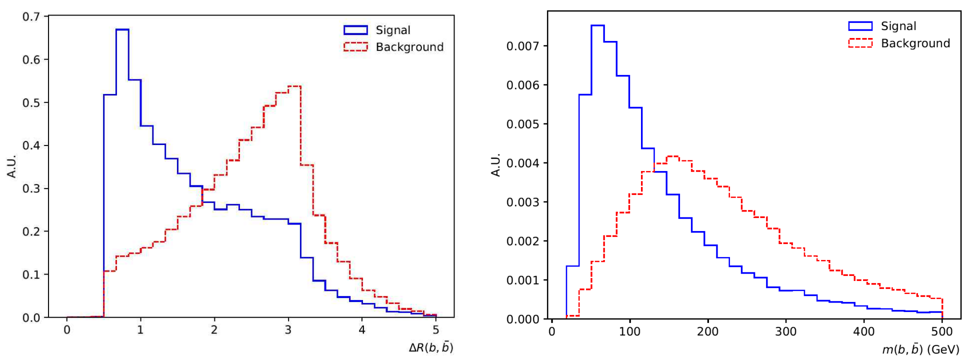

Figure 3.3 Signal and Background Plots of ΔR (left), Invariant mass (right)

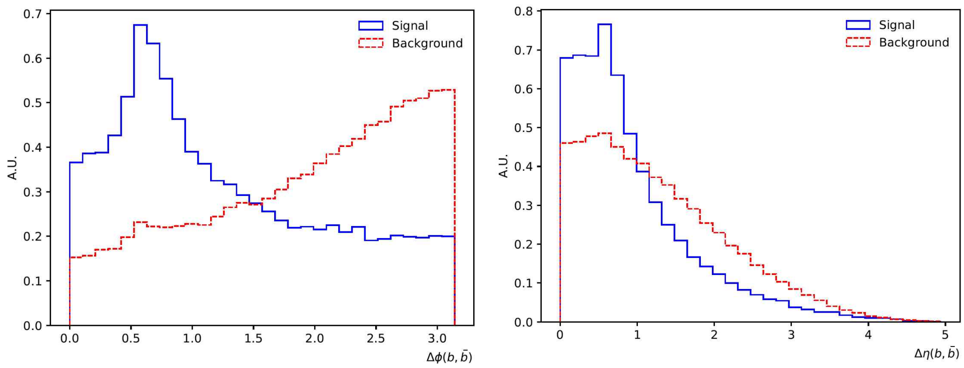

Figure 3.4 Signal and Background Plots of $\Delta\phi$ (left), $\Delta\eta$ (right) of two b-jets

Figure 3.3 and 3.4 are plots of some input variables. These input variables are significantly distinguishable between signal and background. We expect to obtain higher performance when signal and background are well distinguishable. Signal is defined as two reconstruction b-jets which are from generated additional b-jets. Other combinations are regarded as background events.

Hyperparameters are deep learning variables, but different from input variables. Node, layer and epoch are representative hyperparameters and they consist deep neural network. We can manipulate those hyperparameters when we conduct deep learning. At the figure 3.2, we can increase the number of hidden layer and nodes which are expressed as a circle in the figure. Epoch is the number of iterations to use dataset in deep learning.

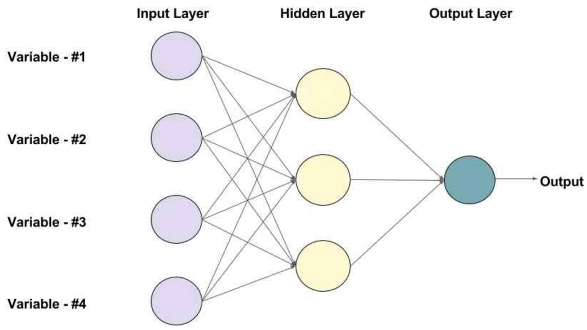

Figure 3.5 Deep Neural Network [14]

Deep Learning Environment	
Using Keras backend Tensorflow	
Activation Function	ReLU
Loss	Binary Cross Entropy
Optimizer	Adam
Batch size	1024
Input Variables	78 variables

Table 3.2 Deep Learning Environments

Deep learning environments are listed in Table 3.1. With this environment, we train the data with given signals and test with test sets which are different from training data. When training the data, 80% of our event samples were used for each selection and remaining 20% were used to test the trained model. In this regard, reconstruction efficiency is the ratio of test matched events and total test events. For every epoch, we calculated reconstruction efficiency using test events and choose the best model with the highest reconstruction efficiency. To optimize hyperparameters, fixing the number of epochs to 100, we varied the number of nodes and layers. As an example, heatmaps of hyperparameter optimization for the requirements of b-jets $\geq$ 4 are shown in Figure 3.6.

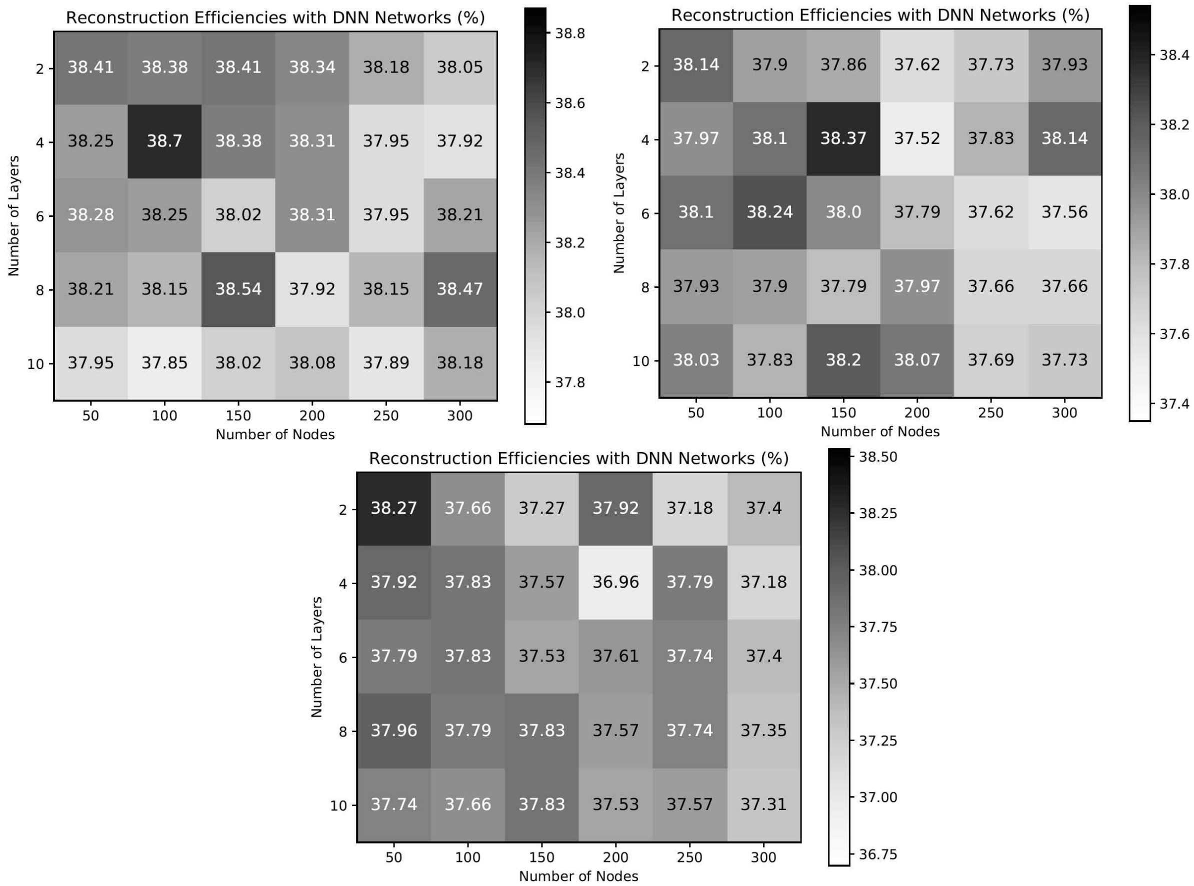

Figure 3.6 Hyperparameter Optimization for b-Jets ≥ 4
Jets ≥ 4 (upper left), Jets ≥ 5 (upper right), Jets ≥ 6 (lower)

From the Figure 3.6, we can figure out that the smaller number of nodes and layers performs better in the smaller number of events. However, when the number of events is enough to perform deep learning, the best nodes and layers that have the highest reconstruction efficiency is random by event selections. Therefore, we fixed the number of nodes and layers to 100 and 4 respectively and increased epochs to 500 for optimize the number of epochs.

Number of Jets	Number of b-Jets	Best Epoch	Test Matched Events	Total Test Events	Reconstruction efficiency (%)
≥ 2	≥ 2	349	12406	55025	22.55
	≥ 3	488	12355	54733	22.57
	≥ 4	85	11773	51944	22.66
	≥ 5	386	9723	42689	22.78
	≥ 6	210	6297	27429	22.96
≥ 3	≥ 3	235	6007	18394	32.66
	≥ 4	256	5903	18039	32.72
	≥ 5	201	5196	15899	32.68
	≥ 6	137	3606	11089	32.52
≥ 4	≥ 4	26	1192	3067	38.87
	≥ 5	53	1109	2929	37.86
	≥ 6	30	872	2297	37.96

Table 3.3 Deep Learning Results

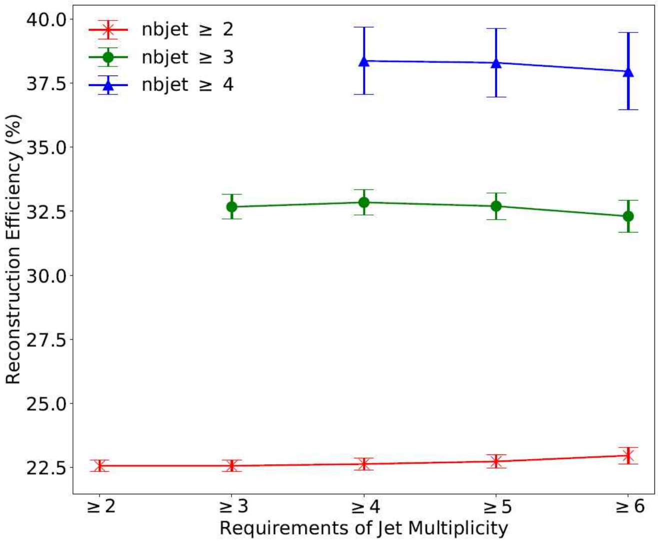

Figure 3.7 Deep Learning Results

Table 3.3 and Figure 3.7 are the results of deep learning. As like the minimum ΔR method, when the event selections become tighter, the reconstruction efficiency increases. Here, we will focus on the results of jets ≥ 6 and b-jets ≥ 3 because the process requires 6 jets and 4 b-jets. If we choose b-jets ≥ 4, the number of selected events is too small thus it can cause statistical error.

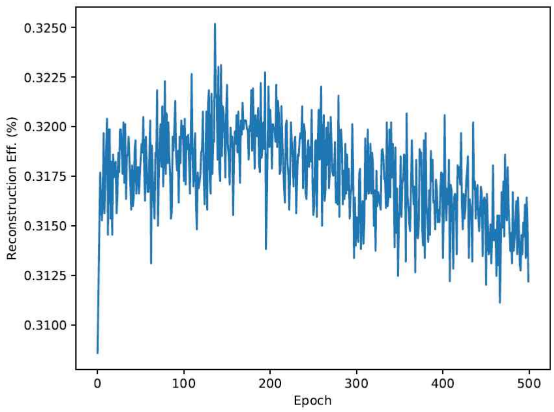

Figure 3.8 Reconstruction Efficiencies for each epochs of jets≥6 and b-jets≥3 selection

In the Figure 3.8, the reconstruction efficiency is the highest at the epoch 137. After the peak at epoch 100~200, the reconstruction efficiency decreases, and overtraining occurs.

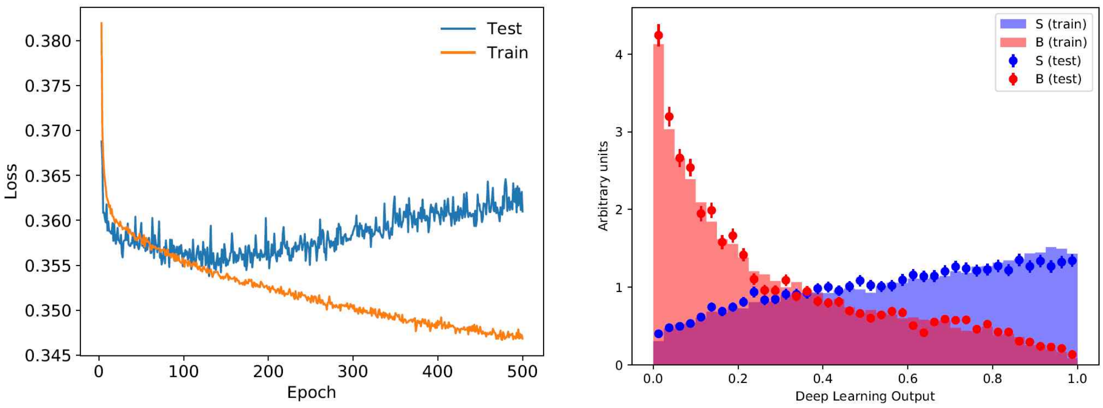

Figure 3.9 Plots for Loss (Left) and Deep Learning Output (Right) for jets≥6 and b-jets≥3

Overtraining check is necessary for deep learning. According to the Figure 3.9, overtraining was not occurred for jets ≥ 6 and b-jets ≥ 3 selection. At the Table 3.3, the best epoch for jets ≥ 6 and b-jets ≥ 3 is 137 and there was no difference between test and train in terms of loss. Also, in the deep learning output plot, test signal and background follow train signal and background well.

4 Conclusion

We used two method to identify the two additional b-jets. Comparing those methods in Figure 4.1, deep learning method has higher reconstruction efficiency than minimum ΔR method. Also, for each minimum ΔR method and deep learning method, when the number of b-jets cut is tighter, reconstruction efficiency increases significantly. The ratio of signal and background events affected on the performance for each method. Looser event selection has lower reconstruction efficiency and tighter event selection has higher reconstruction efficiency.

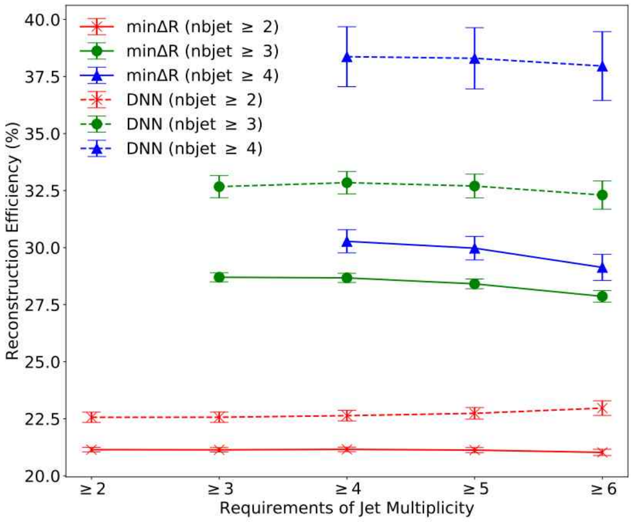

Figure 4.1 Comparison between Minimum ΔR Method and Deep Learning

From this result, we expect to obtain higher reconstruction efficiencies with CMS experiment data using deep learning. Also, we would be able to remove the $t\bar{t}b\bar{b}$ process better within other important processes, $t\bar{t}H(b\bar{b})$ or $tcH(b\bar{b})$ process. Finally, we can better understand about top quark, Higgs boson, FCNC and other physics.

Acknowledgement

For a year of the $t\bar{t}b\bar{b}$ study, I want to express to the graduation thesis director, Professor Tae Jeong Kim. In 2018, I chose him as my graduation thesis director, and he gave me a lot of chances to get familiar with particle physics. Some activities in particle physics subject helped me a lot to better understand the physics. Also, as a tutor assistant, Jieun Choi in Elementary Particle Physics Laboratory gave me continuous feed-back for several technical problems.

Reference

[1] The accelerator complex. (n.d.). Retrieved April 26, 2019, from https://home.cern/science/accelerators/accelerator-complex

[2] The Large Hadron Collider. (n.d.). Retrieved from https://home.cern/science/accelerators/large-hadron-collider.

[3] Picture from https://cds.cern.ch/record/1621583/files/CERN%27s-accelerator-complex2013.jpg?version=1

[4] CMS. (n.d.). Retrieved October 23, 2019, from https://home.cern/science/experiments/cms.

[5] Picture from https://twiki.cern.ch/twiki/pub/CMSPublic/SketchUpCMSGallery/cms_160312_02.png

[6] Picture from http://inspirehep.net/record/1236817/files/img_cms_coordinates.png

[7] Albajar, C., Albrow, M. G., Allkofer, O. C., Astbury, A., Aubert, B., Axon, T., ... & Bauer, G. (1988). Measurement of the bottom quark production cross section in proton-antiproton collisions at√ s= 0.63 TeV. *Physics Letters B*, *213*(3), 405-412.

[8] Alwall, J., Frederix, R., Frixione, S., Hirschi, V., Maltoni, F., Mattelaer, O., ... & Zaro, M. (2014). The automated computation of tree-level and next-to-leading order differential cross sections, and their matching to parton shower simulations JHEP07 (2014) 079. *arXiv preprint arXiv:1405.0301*.

[9] Artoisenet, P., Frederix, R., Mattelaer, O., & Rietkerk, R. (2013). Automatic spin-entangled decays of heavy resonances in Monte Carlo simulations. *Journal of High Energy Physics*, *2013*(3), 15.

[10] Sjöstrand, T., Mrenna, S., & Skands, P. (2008). A brief introduction to PYTHIA 8.1. *Computer Physics Communications*, *178*(11), 852-867.

[11] De Favereau, J., Delaere, C., Demin, P., Giammanco, A., Lemaitre, V., Mertens, A., ... & Delphes 3 Collaboration. (2014). DELPHES 3: a modular framework for fast simulation of a generic collider experiment. *Journal of High Energy Physics*, *2014*(2), 57.

[12] Picture from Bartosik, N. (2015). Associated Top-Quark-Pair and b-Jet Production in the Dilepton Channel at $₩sqrt {s} $= 8 TeV as Test of QCD and Background to tt+ Higgs Production (Doctoral dissertation, DESY).

[13] Jo, Y. K., Choi, S. Y., Roh, Y. J., & Kim, T. J. (2015). Study of the top-quark pair production in association with a bottom-quark pair from fast simulations at the LHC. Journal of the Korean Physical Society, 67(5), 807-812.

[14] Picture from https://www.learnopencv.com/understanding-feedforward-neural-networks/

Appendix 1. Deep Learning Input Variables

Here is the list of input variables used in deep learning. b-jet 1 in the list has the highest p_T and b-jet 2 is the second highest p_T. W is a pair of two jets (not b-jets) that has the nearest mass with W-boson.

Variables	Properties
$p_{T,1}$	Transverse momentum of b-jet 1
η_1	Pseudo-rapidity of b-jet 1
E_1	Energy of b-jet 1
$p_{T,2}$	Transverse momentum of b-jet 2
η_2	Pseudo-rapidity of b-jet 2
E_2	Energy of b-jet 2
ΔR_{bb}	ΔR of two b-jets
$\Delta\eta_{bb}$	$\Delta\eta$ of two b-jets
$\Delta\phi_{bb}$	$\Delta\phi$ of two b-jets
$p_{T,bb}$	Transverse momentum of two b-jets
η_{bb}	Pseudo-rapidity of two b-jets
m_{bb}	Invariant mass of two b-jets
$H_{T,bb}$	Scalar sum of transverse momentum of two b-jets
$m_{T,bb}$	Transverse mass of two b-jets
ΔR_{lbb}	ΔR of a lepton and two b-jets
$\Delta\eta_{lbb}$	$\Delta\eta$ of a lepton and two b-jets
$\Delta\phi_{lbb}$	$\Delta\phi$ of a lepton and two b-jets
$p_{T,lbb}$	Transverse momentum of a lepton and two b-jets
η_{lbb}	Pseudo-rapidity of a lepton and two b-jets
m_{lbb}	Invariant mass of a lepton and two b-jets
$H_{T,lbb}$	Scalar sum of transverse momentum of a lepton and two b-jets
$m_{T,lbb}$	Transverse mass of a lepton and two b-jets
ΔR_{lb1}	ΔR of a lepton and b-jet 1
$\Delta\eta_{lb1}$	$\Delta\eta$ of a lepton and b-jet 1
$\Delta\phi_{lb1}$	$\Delta\phi$ of a lepton and b-jet 1
$p_{T,lb1}$	Transverse momentum of a lepton and b-jet 1
η_{lb1}	Pseudo-rapidity of a lepton and b-jet 1
m_{lb1}	Invariant mass of a lepton and b-jet 1
$H_{T,lb1}$	Scalar sum of transverse momentum of a lepton and b-jet 1
$m_{T,lb1}$	Transverse mass of a lepton and b-jet 1
ΔR_{lb2}	ΔR of a lepton and b-jet 2
$\Delta\eta_{lb2}$	$\Delta\eta$ of a lepton and b-jet 2
$\Delta\phi_{lb2}$	$\Delta\phi$ of a lepton and b-jet 2
$p_{T,lb2}$	Transverse momentum of a lepton and b-jet 2
η_{lb2}	Pseudo-rapidity of a lepton and b-jet 2
m_{lb2}	Invariant mass of a lepton and b-jet 2
$H_{T,lb2}$	Scalar sum of transverse momentum of a lepton and b-jet 2
$m_{T,lb2}$	Transverse mass of a lepton and b-jets 2
$\Delta R_{\nu bb}$	ΔR of MET and two b-jets
$\Delta\eta_{\nu bb}$	$\Delta\eta$ of MET and two b-jets
$\Delta\phi_{\nu bb}$	$\Delta\phi$ of MET and two b-jets
$p_{T,\nu bb}$	Transverse momentum of MET and two b-jets
$\eta_{\nu bb}$	Pseudo-rapidity of MET and two b-jets
$m_{\nu bb}$	Invariant mass of MET and two b-jets

Table A1.1 Deep Learning Variables

Variables	Properties
$H_{T,\nu bb}$	Scalar sum of transverse momentum of MET and two b-jets
$m_{T,\nu bb}$	Transverse mass of MET and two b-jets
$\Delta R_{\nu b1}$	ΔR of MET and b-jet 1
$\Delta\eta_{\nu b1}$	$\Delta\eta$ of MET and b-jet 1
$\Delta\phi_{\nu b1}$	$\Delta\phi$ of MET and b-jet 1
$p_{T,\nu b1}$	Transverse momentum of MET and b-jet 1
$\eta_{\nu b1}$	Pseudo-rapidity of MET and b-jet 1
$m_{\nu b1}$	Invariant mass of MET and b-jet 1
$H_{T,\nu b1}$	Scalar sum of transverse momentum of MET and b-jet 1
$m_{T,\nu b1}$	Transverse mass of MET and b-jet 1
$\Delta R_{\nu b2}$	ΔR of MET and b-jet 2
$\Delta\eta_{\nu b2}$	$\Delta\eta$ of MET and b-jet 2
$\Delta\phi_{\nu b2}$	$\Delta\phi$ of MET and b-jet 2
$p_{T,\nu b2}$	Transverse momentum of MET and b-jet 2
$\eta_{\nu b2}$	Pseudo-rapidity of MET and b-jet 2
$m_{\nu b2}$	Invariant mass of MET and b-jet 2
$H_{T,\nu b2}$	Scalar sum of transverse momentum of MET and b-jet 2
$m_{T,\nu b2}$	Transverse mass of MET and b-jets 2
ΔR_{Wb1}	ΔR of W and b-jet 1
$\Delta\eta_{Wb1}$	$\Delta\eta$ of W and b-jet 1
$\Delta\phi_{Wb1}$	$\Delta\phi$ of W and b-jet 1
$p_{T,Wb1}$	Transverse momentum of W and b-jet 1
η_{Wb1}	Pseudo-rapidity of W and b-jet 1
m_{Wb1}	Invariant mass of W and b-jet 1
$H_{T,Wb1}$	Scalar sum of transverse momentum of W and b-jet 1
$m_{T,Wb1}$	Transverse mass of W and b-jet 1
ΔR_{Wb2}	ΔR of W and b-jet 2
$\Delta\eta_{Wb2}$	$\Delta\eta$ of W and b-jet 2
$\Delta\phi_{Wb2}$	$\Delta\phi$ of W and b-jet 2
$p_{T,Wb2}$	Transverse momentum of W and b-jet 2
η_{Wb2}	Pseudo-rapidity of W and b-jet 2
m_{Wb2}	Invariant mass of W and b-jet 2
$H_{T,Wb2}$	Scalar sum of transverse momentum of W and b-jet 2
$m_{T,Wb2}$	Transverse mass of W and b-jets 2

Table A1.2 Deep Learning Variables (cont'd from Table A1.1)